University of Sistan and Baluchestan

Chemical Process Design

Available online at http://cpd.usb.ac.ir/

Computational Fluid Dynamics Simulation for Predicting Pressure and Velocity Variations at Dry and Two-Phase States in Spinning Cone Column

Iman Khonsha[1]✉

[1]Corresponding Author, Department of Chemical Engineering, Shi.C., Islamic Azad University, Shiraz, Postcode: 71993-1, Iran.
Email: iman.khonsha@iau.ac.ir

ARTICLE INFO

Article type:
Research Article

Article history:
Received: 2025-06-09
Received in revised form: 2025-11-22
Accepted: 2025-11-25
Available online: 2025-11-25

Keywords: *Computational Fluid Dynamics; Spinning Cone Column; Pressure drop; Velocity*

ABSTRACT

Spinning cone distillation column (SCC) is a gas-liquid contacting instrument whose function is in the food processing industries. This technology serves as a complementary approach to conventional packed and plate column distillation, particularly in applications requiring high tolerance to solid contaminants and minimal thermal impact on processed materials. In this research, CFD simulations were conducted using pressure and velocity distributions in a pilot-scale SCC, both in the presence of gas and in the absence of liquid flow (dry column) and in the presence of both gas and liquid (two-phase column). The innovation of this research is the results of the new geometry in the simulation. At the present work, the modeling of four fixed cones and three spinning cones, which is between them, has been performed and the suction effect of the spinning cones at the top and bottom of the tower is also taken into account .This geometry led to more accurate results than the experimental results. An increase in gas flow rate may result in higher pressure drops in both dry and two-phase conditions. By calculating logarithm, the line slope of CFD and experimental data will obtain which is equal to 1.835 and 1.847 respectively. These amounts match with the curve slope of pressure drop regarding passed gas flow velocity from orifice (1.8-2). The simulation results can be used to predict industrial applications of the SCC.

Cite this article: Khonsha, I., (2026), Computational Fluid Dynamics Simulation for Predicting Pressure and Velocity Variations at Dry and Two-Phase States in Spinning Cone Column, *Chemical Process Design*, 5(1), 42-53. http//doi.org/10.22111/cpd.2025.52360.1061

DOI: http//doi.org/10.22111/cpd.2025.52360.1061

Publisher: University of Sistan and Baluchestan.

1. Introduction

The SCC is used in the food industry to separate volatile components from liquids and slurries [1]. The advantages of SCC compared with conventional columns include low liquid hold up, low pressure drop, good multistage capability and ability to handle liquids which contain a high proportion of suspend solids [2]. A spinning cone column

consists of a vertical succession of alternate rotating and stationary cones (Fig. 1). Liquid flows, as a film down the stationary cone, drains into the base of the rotating cone, and moves upwards on the rotating cone again as a film by the action of the centrifugal force. Gas flows, up the column, countercurrent to the flow of the liquid. Mass transfer from the liquid to the vapor phase in a SCC takes place through the large surface area of the film (which may be less than 1mm thick), and through the liquid spray in the regions between spinning and stationary cones [3]. The thickness of the film and the shape of its surface are among the key parameters affecting the mass and the momentum transfer from the liquid to the vapor phase [4]. The correlations for pressure drop and flooding limit, developed for conventional packed and plate distillation columns, are largely inapplicable here due to the specific, rotation-related design of SCCs [5].

Since 1995, research work has aimed to understand, on a fundamental basis, the physical processes in spinning cone columns and to create a comprehensive mathematical model of SCC functioning. This has led to the development of a model for liquid film flow on rotating conical surfaces and the creation of the first Computational Fluid Dynamics (CFD) model of an SCC [6]. Makarytechev et al. and Zivdar et al. presented the most recent investigations regarding prediction in SCC with CFD evaluation. Makarytechev et al. accomplished simulation of flow model and pressure distribution in dry SCC Column with laboratory scale in 2002 and 2003 [1, 3]. In 2004, the evaluation of liquid dispersion consequences on pressure drop with CFD and its comparison with the estimations of air– water system at 1000rpm rotor speed were performed by Makarytechev et al. [7]. In 2004, Zivdar et al. explored the hydrodynamics gas flow in the absence of liquid flow by using CFD analysis in laboratory scale [8].

In 2005, Makarytechev et al. examined the outcome of scale up on SCC columns in small, medium and large scales by utilizing CFD simulation [9]. The estimations on the mass transfer parameters inclusive of liquid film thickness, gas and liquid side mass transfer coefficients and HETP for steam stripping of ethanol/water solution were performed in pilot scale by Zivdar et al. in 2009 [10]. In 2010, reconsideration of the current studies regarding CFD analysis of SCC columns was generally performed by Zivdar et al. [11]. Saghatoleslami et al in 2012 evaluated the flooding limits, pressure drop, the effect of tray speed, cone spacing, flooding for both industrial and small scale and predict tower capacity using neural networks. Furthermore, variation of gas and liquid flow rate in an industrial scale spinning cone column has also been studied [12].

In a recent study by Zivdar et al., the pressure drop parameter of the air system inside the SCC tower was investigated on a pilot scale using computational fluid dynamics and compared with experimental data. The model in this study included two stages of the tower and the dry and two-phase pressure drop parameters were reported at rotational speeds of 500, 1000, and 1500rpm. The effect of rotational speed on the pressure drop inside the tower was also investigated. The average relative error in the dry pressure drop case is 11% and for the two-phase pressure drop data at liquid flow rates of 0.6, 0.9, and 1.5 kg/min, it is 13%. The simulation results also show that with increasing rotation speed, the system pressure drop also increases [13]. In a new study, fluid dynamics inside a lab-scale SCC are investigated from a new angle. Full three-dimensional CFD transient simulations are conducted under various operation and design conditions. In particular, an Eulerian-Lagrangian approach is implemented to describe the motions of the liquid droplets as well as of the liquid film. Based on the results from the CFD simulations, key phenomena for the enhanced performance in monomer removal by the SCC are discussed [14]. The purpose of the present work is to examine parameters of dry and two-phase pressure drops and velocity for SCC in Pilot scale by CFD, and to differentiate them with experimental data. The intended geometry consists of three spinning cones and

four fix cones. The innovation of this research is the results of the new geometry in the simulation. At the present work, the modeling of four fixed cones and three spinning cones, which is between them, has been performed and the suction effect of the spinning cones at the top and bottom of the tower is also taken into account .This geometry led to more accurate results than the experimental results. In order to decrease mesh number and to reduce the calculation time, 90 degrees of column has been considered symmetrically. The advantages of this simulation for predicting industrial applications of SCC contain evaluation of the pressure drop parameters, flooding, column efficiency and designing the diameters of SCC column.

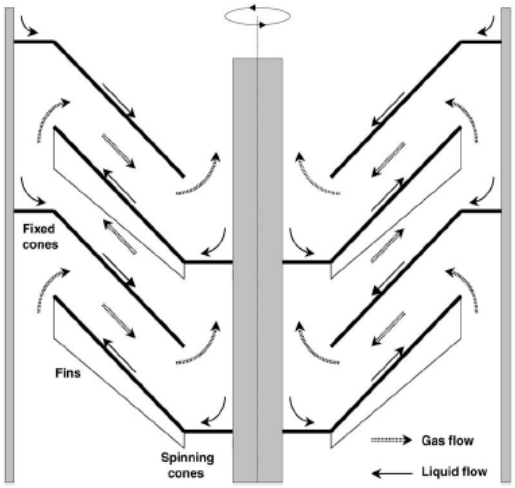

Fig. 1. Flow passage of liquid and gas in SCC [15, 16]

2. Geometry and modeling

Table 1 and Fig. 2 demonstrate geometrical parameters of the column whose scale is pilot. This paper evaluates four fixed cones and three spinning cones, which are between them. According to Fig. 3 tetrahedrons, prisms and pyramids were types of employed meshes which were equal to 309306, 209223 and 5618, respectively, whose total numbers were 524147 elements. Fig. 4 shows the pressure variations in the radial distance between the rotating and stationary intermediate trays at different mesh sizes. This figure presents that while utilizing 5mm mesh size, there would be independency occurrence of the mesh and the hydrodynamic variations were constant.

Table1. Geometrical parameters of SCC [7]

Parameter	Value
Spinning Cone	
Inner radius, R_{SI} (m)	0.0525
Outer radius, R_{SO} (m)	0.145
Fixed Cone	
Inner radius, R_{FI} (m)	0.05
Outer radius, R_{FO} (m)	0.1725
Column	
Shell inner radius, R_C (m)	0.1735
Shaft radius, R_S (m)	0.0325
Cone pitch, P_C (m)	0.04
Number of cone sets, N	30
Spacing parameter, B(m)	03535
Cone angle, Θ (°)	45

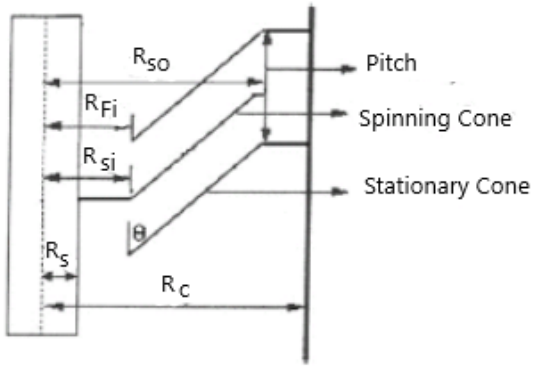

Fig. 2. Geometry of a section of SCC consisting one spinning cone and two fix cones

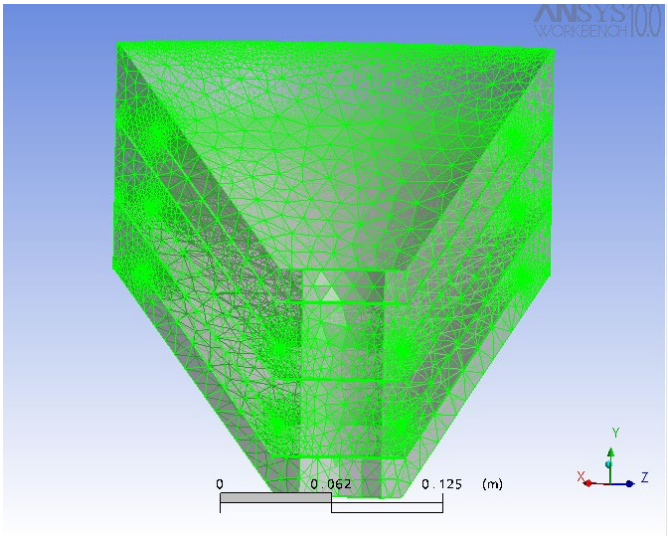

Fig. 3. Meshed geometry of a section of SCC consisting three spinning cone and four fix cones

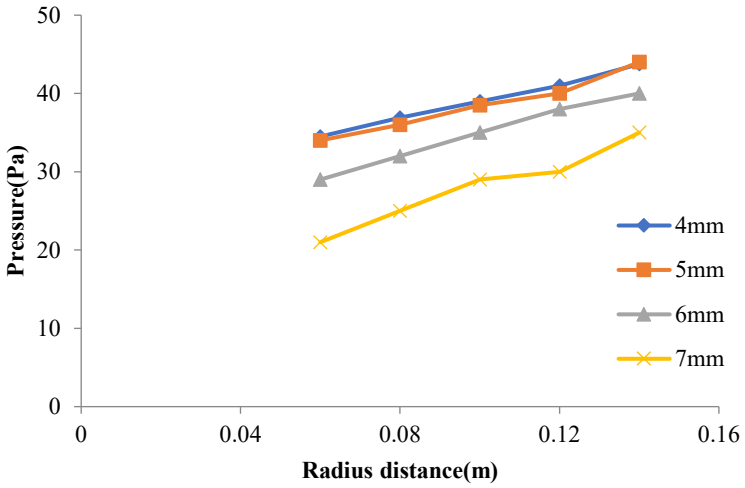

Fig. 4. Analyzing mesh independency along the spinning surface cone

Equations of continuity, momentum, energy, and mass transfer are applied in order to construct mathematical modeling of fluid flow. The column temperature is assumed constant, as the objective of this study is to evaluate hydrodynamic parameters such as pressure drop and velocity. Thereby assessing the energy equations is not necessary. But given the direct relationship between temperature and pressure, it can be assumed that increasing

temperature has a direct effect on increasing tower pressure. Furthermore, the mass transfer equations are ignored as a result of supposing low mass transfer between phases. Therefore, only the continuity and momentum (Navier-Stokes) equations were used in the simulation. A stationary axisymmetric liquid flow over a rotating conical surface in a spherical system of coordinates rotating with constant angular velocity ω may be described by the Navier-Stokes and continuity equations. In the boundary layer approximation (the film thickness δ is much smaller than the radial distance r), these relations can be utilized as incompressible and Newtonian forms which can be simplified to [16]:

$$u_r \frac{\partial u_r}{\partial r} + \frac{u_\theta}{r}\frac{\partial u_r}{\partial \theta} - \frac{(u'_\varphi)^2}{r} - \omega^2 r \sin^2\theta + 2\omega u'_r \sin\theta = -g\cos\theta + \frac{v}{r^2}\frac{\partial^2 u_r}{\partial \theta^2} \tag{1}$$

$$-u_r \frac{\partial u'_\varphi}{\partial r} - \frac{u_\theta}{r}\frac{\partial u'_\varphi}{\partial \theta} - \frac{u_r u'_\varphi}{r} + 2\omega u_r \sin\theta = -\frac{v}{r^2}\frac{\partial^2 u'_\varphi}{\partial \theta^2} \tag{2}$$

$$-(u'_\varphi)^2 \frac{\cot\theta}{r} - \omega^2 r \sin\theta\cos\theta + 2\omega u'_\varphi \cos\theta = -g\sin\theta - \frac{1}{\rho r}\frac{\partial p}{\partial \theta} \tag{3}$$

$$\frac{\partial u_r}{\partial r} + 2\frac{u_r}{r} + \frac{1}{r}\frac{\partial u_\theta}{\partial \theta} = 0 \tag{4}$$

where the tangential velocity in rotating coordinates is $u'_\varphi = u_\varphi + \omega r \sin\theta$.

In the state equations, p refers to the pressure, u_r, u_θ, u_φ are relevant to radial, meridional and tangential velocities of the liquid flow respectively, besides v pertains to the kinematics viscosity. Densities of air and water were equal to 1.185kg/m^3 and 996kg/m^3, respectively, whose function were as the gas and liquid phases. The Grace model, suitable for air-water systems, was applied to calculate the drag force [17]. The SIMPLEC (Semi-implicit Method for Pressure Linked Equation) algorithm is a Trial-and-error method for pressure calculation. The equations were analyzed at 25°C, and the model was solved under steady-state conditions. The simulations used the CFD software CFX-10, which employs a finite volume method to discretize the Navier–Stokes equations. The actual three-phase flow system (continuous liquid film, dispersed liquid droplets, and gas) has been modeled using an Eulerian two-phase (dispersed liquid and gas) CFD model of the column with the geometry and the boundary conditions based on consideration of all three phases.

In Eulerian view, each phase has a specific flow line, and the relation between the phases is illustrated by basic and secondary equations [17]. Pressure drop in the column is supposed linear: according to this assumption, pressure drop can be obtained for one stage of the column and then generalized for the whole column. Gas and liquid flows are steady in the column: as default, these flows are considered steady in the present simulation, which is not steady in reality. Turbulence in gas phase and dispersed liquid phase was state by the standard k-ε model and the zero-equation model, respectively, since the gas and liquid flows in dry and two-phase states were determined turbulent [18]. Although turbulence is inherently unsteady, the steady-state assumption is justified as the model solves for time-averaged flow fields, which are sufficient to capture the mean flow behavior within the spinning cone column [19].

This system has the boundary conditions which contain:

The green areas in Fig. 5, parts (a) to (d), represent the desired boundary conditions.

1. The fix section incorporates fix cones and walls which are stationary according to Fig. 5(a).
2. The rotating section is comprised of spinning cone, fin and rotating shaft, as shown in Fig. 5(b). Calculations of dry and two-phase models are executed at 1000rpm rotation speed.

3. Symmetric section includes 90 degrees of the column, whose goal is to diminish the number of calculations by symmetry which is shown in Fig. 5(c).
4. The bottom flow area is the surface between the down fix cone edge and the shaft, as represented in Fig. 5(d). In this section for the dry case, the input flow rate of gas and for the two-phase case, the speed of input gas and output liquid are given.
5. The above flow area is the surface between the above fix cone edge and shaft, according to Fig. 5(d). In this section, the input flow rate of gas and the speed of input gas and output liquid are assigned for the dry and the two-phase cases, respectively. The outlet pressure in both dry and two-phase states was considered to be 101325pa.

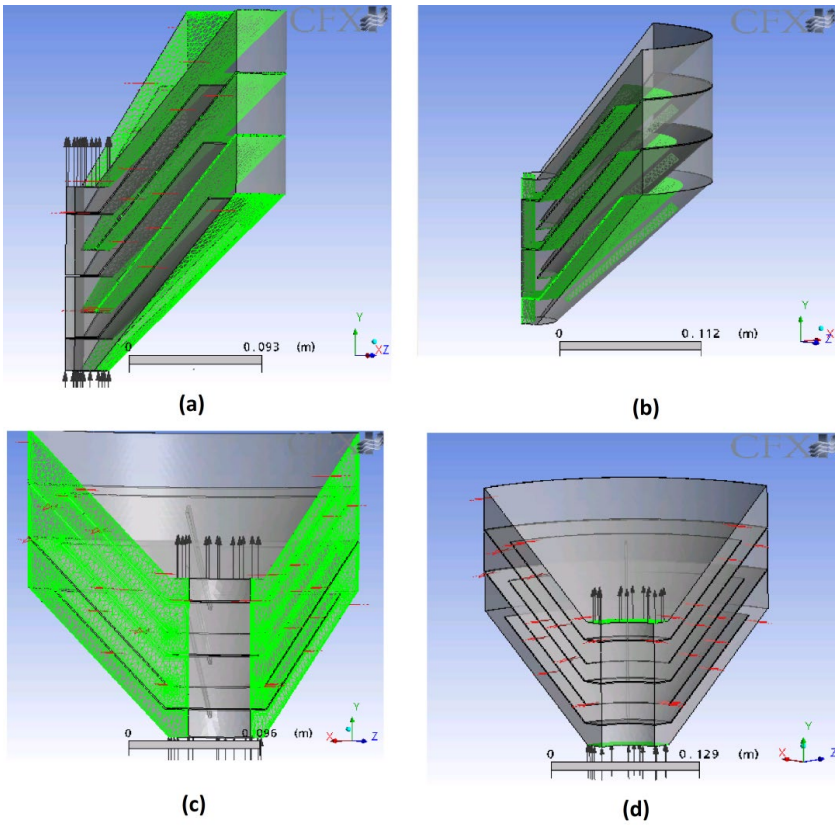

Fig. 5. Boundary conditions: (a) Fix cones, (b) Spinning cones, fins and Shaft (rotational section), (c) Symmetric section, (d) Up and down section

3. Results and discussion

As presented in Fig. 6, pressure drop is predicted by estimating the average pressure drop for one stage, and measuring the pressure drop of the column according to the Eq. (5).

$$N * \Delta p_{stage} = \Delta p \tag{5}$$

In which N represents the number of stages (cone sets) in SCC, Δp_{stage} stand for the pressure drop of one stage and Δp denotes the overall pressure drop through the column.

3.1. Single phase

Fig. 7 shows the velocity vector of the gas phase at 1000rpm and 90lit/min flow rate. From this figure, it can be realized that gas speed is increasing under the influence of rotating section, and this increase is shown by green color.

At Fig. 8 the variations of gas velocity on the spinning cones at 1000rpm and 90lit/min gas flow rate has been inspected. As claimed by this figure, the more radial distance increases, under the influence of rotating section, air flow velocity will get more.

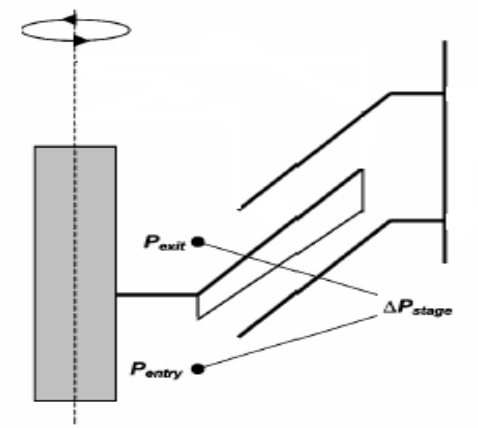

Fig. 6. Pressure drop for one stage [6]

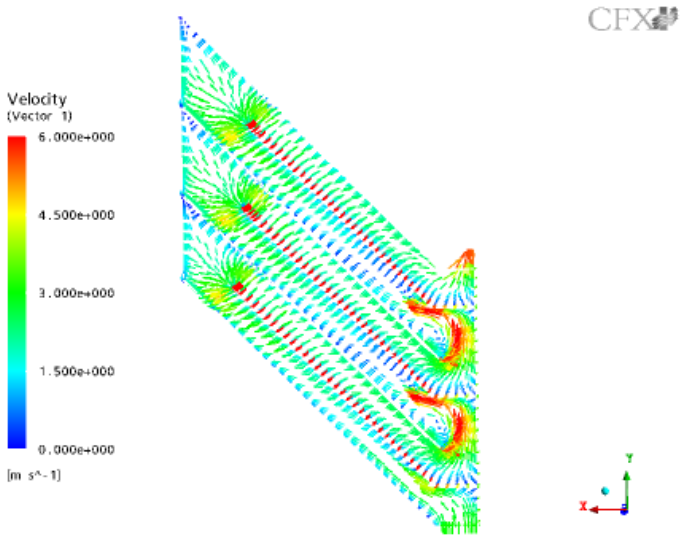

Fig. 7. Air velocity vector at 1000rpm and 90lit/min flow rate in single phase

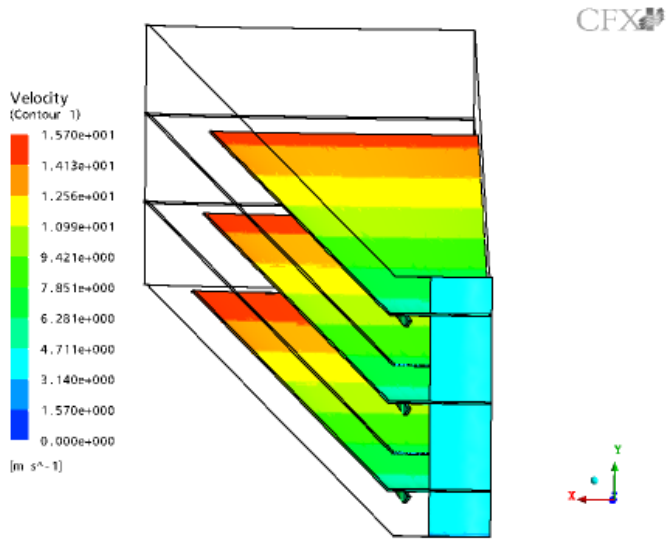

Fig. 8. Air velocity contour at1000rpm and 90 (lit/min) gas flow rate on spinning cones

Pressure contours at 1000rpm and 90lit/min gas flow rate are displayed at Fig. 9, in which high pressure and low pressure areas are represented by the red and blue colors, respectively. On the report of this figure, through rising from the model, the pressure within it will decrease because of the suction caused by spinning of the cones.

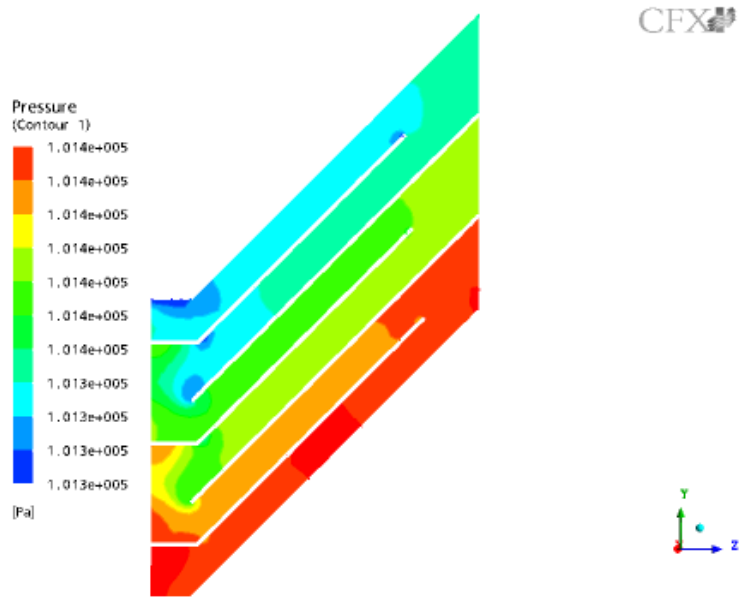

Fig. 9. Dry pressure drop contour at1000rpm and 90 (lit/min) gas flow rate

At Fig. 10, the curve of variant amounts of dry pressure drop at 1000rpm rotating speed has been drawn in terms of different velocities of input gas flow for CFD and experimental results at logarithmic scale. In order to calculate the input or output flow velocity, the gas flow rate is divided to flow area in the input or output which is equal to $0.004m^2$. The fitted equations of the pass lines from CFD and experimental data at Fig.10 are as $y=30.37e^{1.835x}$ and $y=35.00e^{1.847x}$, respectively. By calculating logarithm from the parts of above equations, the line slope of CFD and experimental data will obtain which is equal to 1.835 and 1.847 respectively. These amounts (1.835 and 1.847) match with the curve slope of pressure drop regarding passed gas flow velocity from orifice (1.8-2).

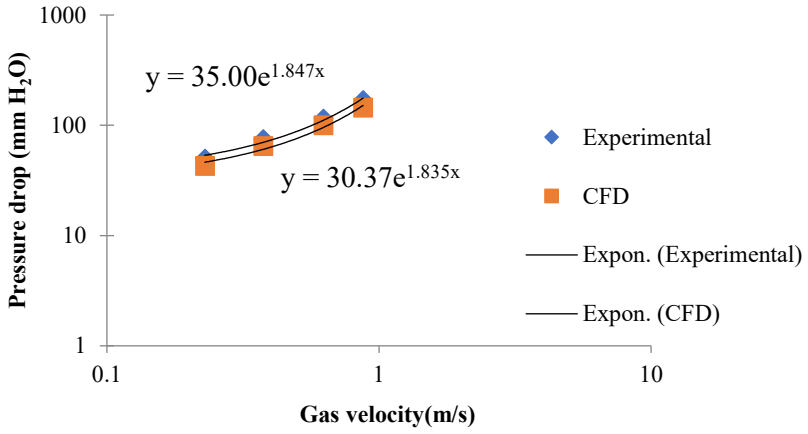

Fig. 10. Comparison of the slop curve for CFD and experimental results [20]

3.2. Two phase

Fig. 11 shows the liquid velocity vectors at 1000rpm and 90lit/min and 0.6lit/min gas and liquid flow rates, respectively, in which dispersion in the liquid flow increases especially at the edge of cone.

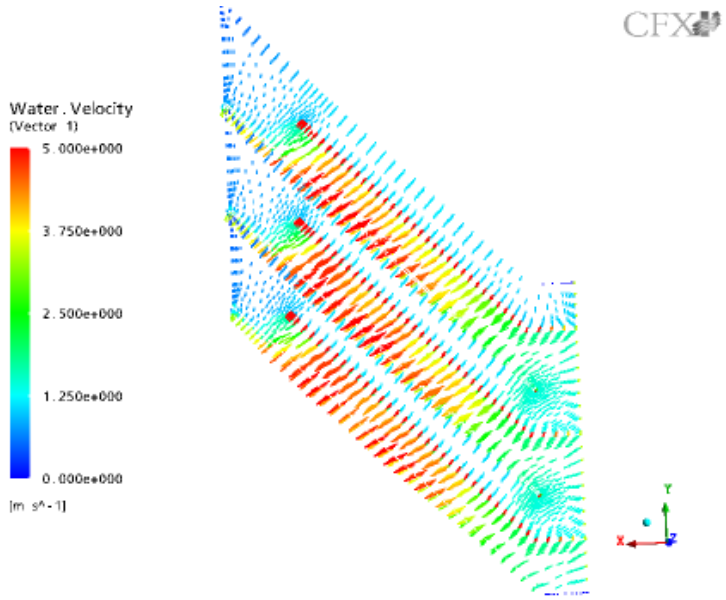

Fig. 11. Liquid velocity vector at 1000rpm and 90lit/min gas flow rate and 0.6lit/min liquid flow rate

Fig. 12 investigates the variations of liquid velocity on the spinning cones at 1000rpm and gas and liquid flow rates of 90lit/min and 0.6lit/min, respectively. As claimed by this figure, the more radial distance increases, under the influence of rotating section, water flow velocity will get more.

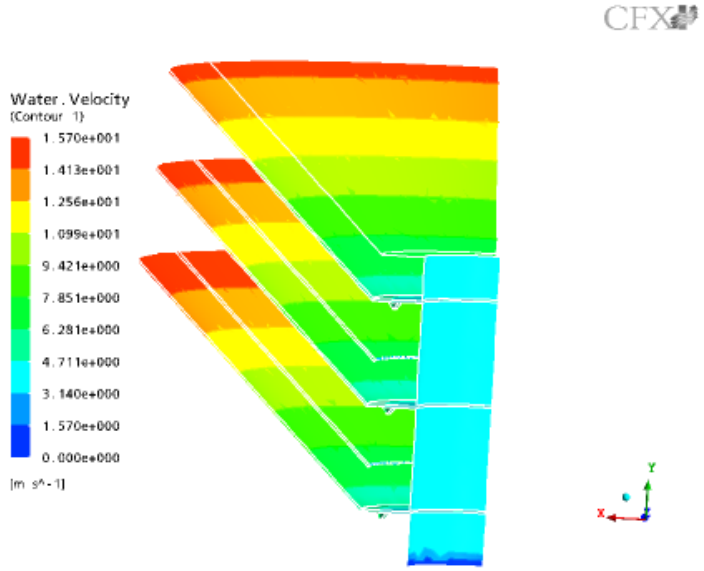

Fig. 12. Water velocity contour at 1000rpm and 90 lit/min gas flow rate and 0.6lit/min liquid flow rate on spinning cones

Fig. 13 shows the water volume fraction for the binary system of 90(lit/min) and 0.6(lit/min) rates of gas and liquid flows, respectively and 1000rpm, where dispersion of water drops on the cones and especially on the edge of the cones is obvious. The bulk of the gas–liquid mass transfer in a SCC was assumed to occur through the surface of a liquid film flowing over the alternating stationary and rotating cones [19]. Fig.14 presents pressure contours, in which the red color is related to the high-pressure areas and the green color refers to the low ones. On the report of this figure, through rising from the model, the pressure within it will decrease, due to the suction caused by spinning of the cones.

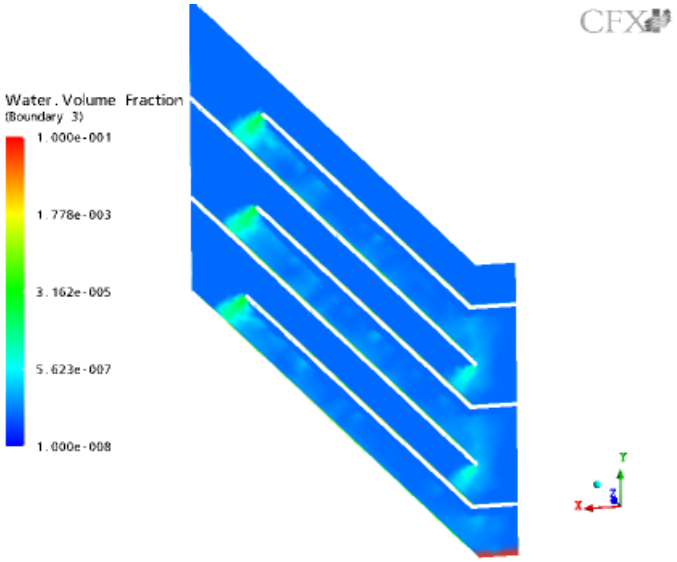

Fig. 13. Water volume fraction for the binary system of water and air at1000rpm and 90lit/min gas flow rate and 0.6lit/min liquid flow rate

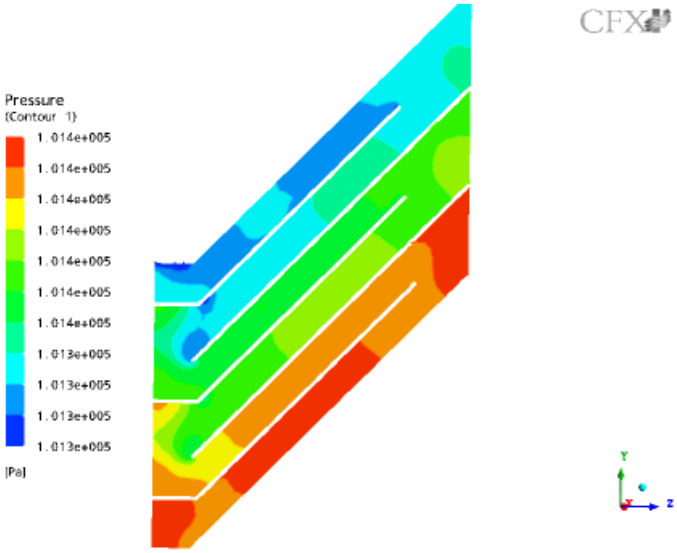

Fig. 14. Two phase pressure drop contour at1000rpm and 90(lit/min) gas flow rate and 0.6(lit/min) liquid flow rate

At Fig. 15, the effects of dry and two-phase pressure drop variations inside the column on 1000rpm rotating speed and different gas flow rates have been investigated and these results have been compared with experimental data. According to this figure, by increasing gas flow rate, the dry and two-phase pressure drop of the column will increase that coordinates with experimental data well. In order to compare the results of the dry and two-phase states, the results were plotted in a graph. In both experimental and simulation results, the difference in pressure drop between dry and two-phase conditions is slight. According to figure, the more gas flow rate increases, at certain liquid flow rate (0.6lit/min), two phase pressure drop will increase whose value is more than pressure drop in dry state. This matter is as a consequence of liquid flow inside the column and reduction of flow area. The results attained by CFD accord with experimental data well.

4. Conclusion

In the present work investigating the pressure drop and velocity in SCC has been performed by CFD simulation. The innovation of this research is the results of the new geometry in the simulation. At the present work, the modeling of

four fixed cones and three spinning cones, which is between them, has been performed and the suction effect of the spinning cones at the top and bottom of the tower is also taken into account. This geometry led to more accurate results than the experimental results. CFD simulation regarded modeling on Eulerian view as two phases of continuous gas and dispersed liquid. Turbulence in the gas phase was modeled using the standard k–ε approach, while the dispersed liquid phase was represented by the zero-equation model.

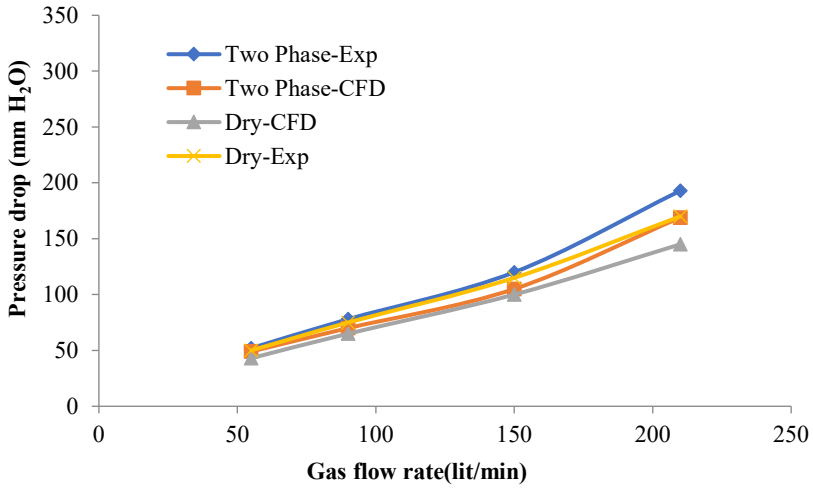

Fig 15. Comparison of simulation and experimental results [20] of dry and two-phase pressure drop at a speed of 1000 rpm and a liquid flow rate of 0.6 lit/min

According to the CFD results There is constancy of hydrodynamic variations, besides the utilized mesh was of unstructured whose independency occurrence was at 5mm. Calculations of the dry and two-phase models were performed at 1000 rpm rotating speed, by which it was confirmed that the more gas flow rate increases, the buoyant effect (gravity force) on the dispersed liquid phase will decrease which causes the fouling increase in flow throats and pressure drop elevation. By increasing the radial distance, air and water flow velocity will expand which is due to the influence of rotating section. The suction generated by the spinning cones makes the pressure within the model decrease. The fitted equations of the pass lines from CFD and experimental data are as $y=30.37e^{1.835x}$ and $y=35.00e^{1.847x}$, respectively.

By calculating logarithm, the line slope of CFD and experimental data will obtain which is equal to 1.835 and 1.847 respectively. These amounts match with the curve slope of pressure drop regarding passed gas flow velocity from orifice (1.8-2). The more gas flow rate increases, at certain liquid flow rate, two phase pressure drop will increase whose value is more than pressure drop in dry state. This matter is as a consequence of liquid flow inside the column and reduction of flow area. The results attained by CFD accord with experimental data well. In both experimental and simulation results, the difference in pressure drop between dry and two-phase conditions is slight, and the two-phase pressure drop is slightly higher than the dry condition. This matter is as a consequence of liquid flow inside the column and reduction of flow area. The results attained by CFD accord with experimental data well.

Nomenclature

Symbols

B	Spacing parameter, the ratio of the vertical distance between the fixed and the spinning cone surfaces to the cone pitch	R_{FI}	Inner radius of the fixed cone (m)
g	Acceleration due to gravity (9.81 ms^{-2})	R_{SO}	Outer radius of the spinning cone (m)

N	Number of stages (cone sets) in SCC	R_{SI}	Inner radius of the spinning cone (m)
P_C	Cone pitch, vertical distance between two successive fixed or spinning cones (m)	U	Real velocity (ms^{-1})
P	Pressure (Pa)	**Greek symbols**	
Δp	Overall pressure drop through the column (Pa)	ν	kinematics viscosity (m^2s^{-1})
Δp_{stage}	Pressure drop of one stage (Pa)	θ	Cone angle, degrees
R_C	Column inner radius (m)	ρ	Density (kgm^{-3})
R_S	Shaft radius (m)	ω_{rot}	Angular velocity of the spinning cone rotation (s^{-1})

Conflict of interest

On behalf of author, the corresponding author states that there is no conflict of interest.

References

[1] Makarytechev, S. V., Langrish, T. A. G., Fletcher, D. F., 2002. CFD Analysis of Spinning Cone Columns: Prediction of Unsteady Gas Flow and Pressure Drop in a Dry Column, Chemical Engineering Journal, 87(3), 301-311. https://doi.org/10.1016/S1385-8947(01)00245-5

[2] Zivdar, M., 1998, Distillation for Food Flavour Separation, PhD Thesis University of Sydney.

[3] Langrish, T. A. G., Makarytechev, S. V., Fletcher, D. F., Prince, R. G. H., 2003. Progress in Understanding the Physical Processes Inside Spining Cone Columns, Chemical Engineering Research and Design, 81(1), 122-130. https://doi.org/10.1205/026387603321158276

[4] Makarytechev, S. V., Langrish, T. A. G., Prince, R. G. H., 2001. Thickness and Velocity of Wavy Liquid Films on Rotating Conical Surfaces, Chemical Engineering Science, 56(1), 77-87. https://doi.org/10.1016/S0009-2509(00)00428-0

[5] Makarytechev, S. V., Langrish, T. A. G., 2005. Pressure Drop and Flooding Limit in Spinning Cone Columns, Chemical Engineering Communications, 192(4), 445-473. https://doi.org/10.1080/00986440590477736

[6] Makarytechev, S. V., Langrish, T. A. G., 2004. Dry Column Approximation for Pressure Drop in Spinning Cone columns, Chemical Engineering Communications, 191(5), 641-664. https://doi.org/10.1080/00986440490275921

[7] Makarytechev, S. V., Langrish, T. A. G., Fletcher, D. F., 2004. Mass Transfer Analysis of Spinning Cone Columns Using CFD, Chemical Engineering Research and Design, 82(6), 752-761. https://doi.org/10.1205/026387604774196037

[8] Zivdar, M., Hedayati, B., 2004. Analysis of Gas Flow in SCC Columns using Computational Fluid Dynamics (CFD), Iranian Chemical Engineering Journal, 11, 26.

[9] Makarytechev, S. V., Langrish, T. A. G., Fletcher, D. F., 2005. CFD Analysis of Scale Effects in Spining Cone Columns, Trans IChemE, 83(8), 951-958. https://doi.org/10.1205/cherd.04160

[10] Zivdar, M., Shirdel, S., 2009. CFD Analysis of Mass Transfer Parameter in SCC Distillation Columns, Journal of Separation Science and Engineering, 1(1), 23-33. https://dor.isc.ac/dor/20.1001.1.20083963.1388.1.1.3.8

[11] Zivdar, M., Shirdel, S., Khonsha, I., Poorjafar, L., 2010. Review of CFD Analysis in Spinning Cone Columns, Iranian Chemical Engineering Journal, 9(46), 31.

[12] Saghatoleslami, N., Amiri, M., Rohigolkhatmi, J., 2012. Prediction of flooding and pressure drop in a spinning cone column using neural networks International, Journal of Industrial Chemistry, 3, 8. https://doi.org/10.1186/2228-5547-3-8

[13] Zivdar, M., Yousefi, M., Shahroi, N., 2021. Hydrodynamic Investigation of Spinning Cone Column by Computational Fluid Dynamics, FarayandNo, 75, 58-70.

[14] Bae, S., Kim, S. H., Lee, J. H., 2019. An investigation into the hydrodynamics of a spinning cone column: CFD simulations by an Eulerian-Lagrangian approach, Computers and Chemical Engineering, 132, 106635. https://doi.org/10.1016/j.compchemeng.2019.106635

[15] Makarytechev, S. V., Langrish, T. A. G., Prince, R. G. H., 1998. Structure and Regimes of Liquid Film Flow in Spinning Cone Columns, Chemical Engineering Science, 53, 1541-1550. https://doi.org/10.1016/S0009-2509(98)00011-6

[16] Khonsha, I., Zivdar, M., Haghshenasfard, M., 2013. Estimation of Hydrodynamic Parameters in Spinning Cone Column Using Computational Fluid Dynamics, Arabian Journal for Science and Engineering, 38, 767–776. https://doi.org/10.1007/s13369-012-0370-7

[17] Makarytechev, S. V., Xue, E., Langrish, T. A. G., Prince, R. G. H., 1997. On Modeling Fluid Flow over a Rotating Conical Surface, Chemical Engineering Science, 52(6), 1055-1057. https://doi.org/10.1016/S0009-2509(96)00473-3

[18] Haghshenasfard, M., 2006. The Design of Packed Column with Structured Packing Using CFD Analysis, PhD Thesis University of Sistan and Baluchestan.

[19] Makarytechev, S. V., Langrish, T. A. G., Fletcher, D. F., 2005. Exploration of Spinning Cone Column Capacity and Mass Transfer Performance Using CFD, Chemical Engineering Research and Design, 83 1372–1380. https://doi.org/10.1205/cherd.03413

[20] Sykes, S.J., Prince, R.G.H., 1991. The Design of Spinning Cone Distillation Columns, Csiro Division of Food Processing.